THE JOURNAL OF BIOLOGICAL CHEMISTRY VOL. 281, NO. 47, pp. 36338–36346, November 24, 2006

Fluorometric Measurements of Intermolecular Distances between the α- and β-Subunits of the Na^+/K^+-ATPase*

Received for publication, May 18, 2006, and in revised form, September 14, 2006 Published, JBC Papers in Press, September 15, 2006, DOI 10.1074/jbc.M604788200

Robert E. Dempski[‡1], Klaus Hartung[‡], Thomas Friedrich[‡§2], and Ernst Bamberg[‡§3]

From the [‡]Department of Biophysical Chemistry, Max Planck Institute of Biophysics, D-60438 Frankfurt am Main and the [§]Biochemistry, Chemistry and Pharmaceutical Sciences Departments, Johann Wolfgang Goethe University Frankfurt, D-60438 Frankfurt am Main, Germany

The Na^+/K^+-ATPase maintains the physiological Na^+ and K^+ gradients across the plasma membrane in most animal cells. The functional unit of the ion pump is comprised of two mandatory subunits including the α-subunit, which mediates ATP hydrolysis and ion translocation, as well as the β-subunit, which acts as a chaperone to promote proper membrane insertion and trafficking in the plasma membrane. To examine the conformational dynamics between the α- and β-subunits of the Na^+/K^+-ATPase during ion transport, we have used fluorescence resonance energy transfer, under voltage clamp conditions on *Xenopus laevis* oocytes, to differentiate between two models that have been proposed for the relative orientation of the α- and β-subunits. These experiments were performed by measuring the time constant of irreversible donor fluorophore destruction with fluorescein-5-maleimide as the donor fluorophore and in the presence or absence of tetramethylrhodamine-6-maleimide as the acceptor fluorophore following labeling on the M3-M4 or M5-M6 loop of the α-subunit and the β-subunit. We have also used fluorescence resonance energy transfer to investigate the relative movement between the two subunits as the ion pump shuttles between the two main conformational states (E_1 and E_2) as described by the Albers-Post scheme. The results from this study have identified a model for the orientation of the β-subunit in relation to the α-subunit and suggest that the α- and β-subunits move toward each other during the E_2 to E_1 conformational transition.

The Na^+/K^+-ATPase is a ubiquitous protein complex that is required for maintaining the concentration gradients of Na^+ and K^+ across the plasma membrane (1, 2). This complex is comprised of two mandatory subunits. The α-subunit is the major catalytic subunit, and the β-subunit is required for proper trafficking of the complex to the plasma membrane (3–5). A third subunit, γ, is also present, at least in certain tissues, which, although not required for function, has been identified as a regulatory protein (6).

The Na^+/K^+-ATPase is one member of more than 200 P-type ATPases, so named because the protein is transiently phosphorylated at a highly conserved aspartate residue upon ATP hydrolysis (7). A series of crystal structures showing different conformational states of a highly homologous P-type ATPase, the sarcoplasmic reticulum Ca^{2+}-ATPase (SERCA),[4] has provided insight into the structure of the Na^+/K^+-ATPase as well as the conformational flexibility of the pump during ion translocation (8–12). It has been demonstrated through these structures that the SERCA pump undergoes significant conformational changes during ion transport. However, as the SERCA pump is comprised of only the α-subunit, no information is available about the involvement of the β-subunit in the conformational flexibility of the Na^+/K^+-ATPase. Direct structural information of the β-subunit has been limited to electron microscopy studies (13, 14). The results from these experiments have proposed a putative location for the β-subunit in relation to the α-subunit. However, this model is inconsistent with some biochemical experiments, and alternative structural models have been proposed (2, 15). Furthermore, as the electron microscopy study yields a static representation of the ion pump, it is difficult to elucidate the relative movements of the α- and β-subunits during ion translocation.

Voltage clamp fluorometry has been recognized as a powerful technique to monitor the conformational dynamics of ion channels (16–18). The method has also been extended to determine distance constraints and the relative movement between protein subunits that accompany gating of the *Shaker* potassium channel and the human glutamate transporter using fluorescence resonance energy transfer (FRET) (19–21). These studies have demonstrated that small scale movements between subunits accompany channel gating.

Our laboratory has previously utilized voltage clamp fluorometry to demonstrate that residues on the α- and β-subunits of the Na^+/K^+-ATPase can be site-specifically labeled with the fluorescent dye tetramethylrhodamine-6-maleimide (TMRM). Fluorescence changes that are induced by changes in membrane potential and/or ion concentrations (Na^+ and/or K^+) can be correlated to the two main conformational states, E_1 and E_2 (Fig. 1*A*), of the Na^+/K^+-ATPase (22, 23).

* The work was supported by the Deutsche Forschungsgemeinschaft (SFB 472), the Max Planck-Gesellschaft zur Föderung der Wissenschaften, and the Johann Wolfgang Goethe-Universität, Frankfurt am Main. The costs of publication of this article were defrayed in part by the payment of page charges. This article must therefore be hereby marked "*advertisement*" in accordance with 18 U.S.C. Section 1734 solely to indicate this fact.

[1] The recipient of a Max Planck fellowship.

[2] Supported by the Federal Ministry of Education and Research (BMBF) program "Unternehmen Region-Innovationsoffensive Neue Länder-Zentren für Innovationskompetenz." Present address: Institute for Chemistry, Technical University of Berlin, D-10623 Berlin, Germany.

[3] To whom correspondence should be addressed. Tel.: 49-69-6303-2001; Fax: 49-69-6303-2222; E-mail: ernst.bamberg@mpibp-frankfurt.mpg.de.

[4] The abbreviations used are: SERCA, sarcoplasmic reticulum Ca^{2+}-ATPase; FRET, fluorescence resonance energy transfer; TMRM, tetramethylrhodamine-6-maleimide; FM, fluorescein-5-maleimide; MOPS, 4-morpholinepropanesulfonic acid; D, donor; A, acceptor.

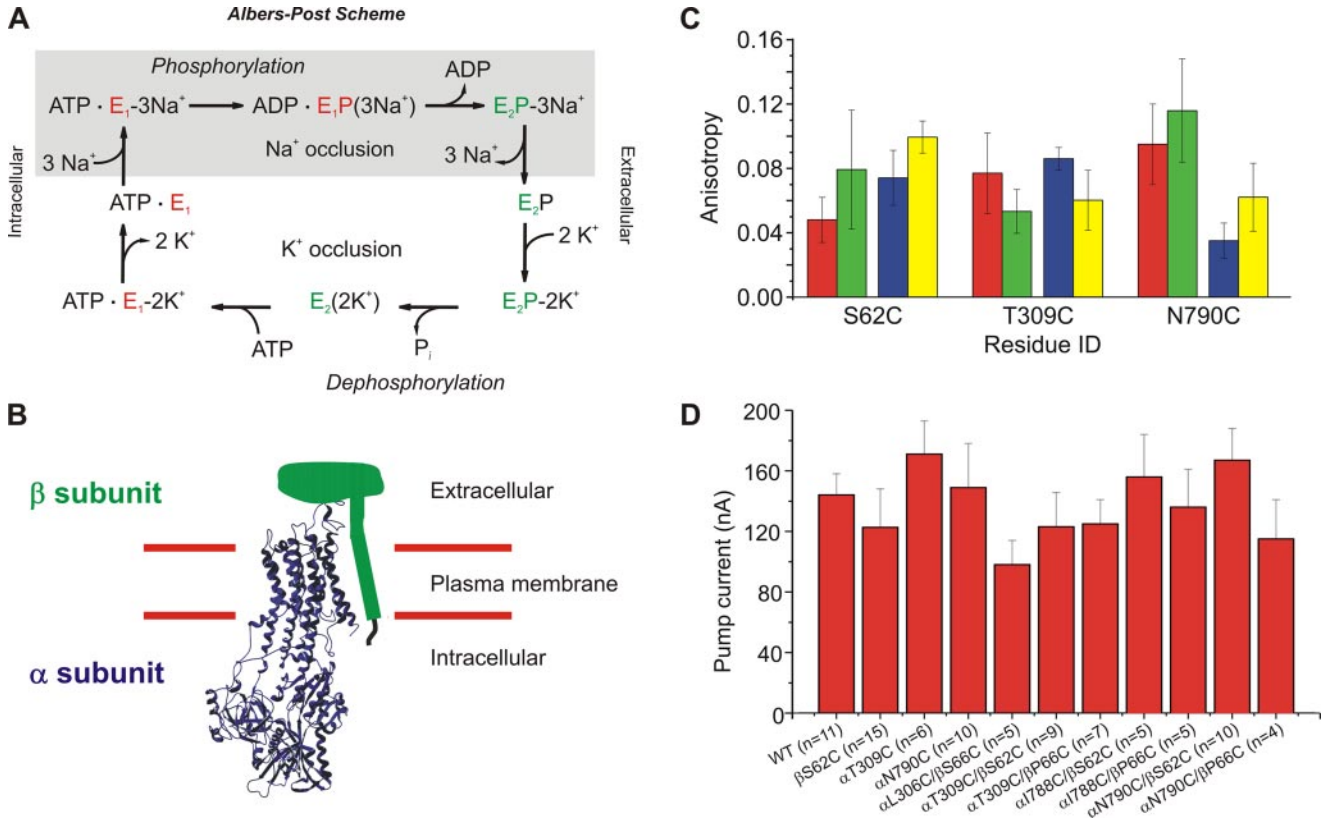

FIGURE 1. **Anisotropic and functional measurements of the Na$^+$/K$^+$-ATPase constructs.** *A*, Albers-Post scheme for the Na$^+$/K$^+$-ATPase reaction cycle. *B*, a schematic diagram of the α- and β-subunits of the Na$^+$/K$^+$-ATPase for donor irreversible photobleaching experiments. The structure of the α-subunit of the Na$^+$/K$^+$-ATPase is modeled into the 1WPE structure from Toyoshima *et al.* (11) using SWISSMODEL (39). *C*, steady state TMRM and FM anisotropy values for different residues of the ion pump in the presence of external Na$^+$ or K$^+$. Color coding is as follows: *red*, TMRM in the presence of external Na$^+$; *green*, TMRM in the presence of external K$^+$; *blue*, FM in the presence of external Na$^+$; and *yellow*, FM in the presence of external K$^+$. All values are given as mean ± S.E. Oocytes were clamped to −20 mV to maintain continuity between anisotropy and donor photodestruction measurements. Data originated from 5–15 oocytes. *D*, stationary pump currents of Na$^+$/K$^+$-ATPase α/β-complexes containing wild- type (*WT*), single-, and double-cysteine mutants from the extracellular M3-M4 or M5-M6 loops of the α-subunit and/or of the β-subunit upon expression in *Xenopus* oocytes at 0 mV holding potential in response to 10 mM K$^+$. Data originated from 4–15 oocytes; values are means ± S.E.

To examine the interaction between the α- and β-subunits of the Na$^+$/K$^+$-ATPase, we have now used voltage clamp fluorometry to determine distance constraints between the α- and β-subunits (Fig. 1*B*). We have also investigated the relative movement between the α- and β-subunits proximal to the extracellular side of the plasma membrane as the ion pump shuttles between the two principle conformational states as described by the Albers-Post scheme, E_1 and E_2 (24, 25). The results from this study have identified the orientation of the β-subunit in relation to the α-subunit and the relative movement of the two subunits during ion transport.

EXPERIMENTAL PROCEDURES

Molecular Biology, Oocyte Preparation, and cRNA Injection—cDNAs of sheep Na$^+$/K$^+$-ATPase α_1-subunit with no extracellular cysteine residues (with mutations C911S and C964A) (26) and reduced ouabain sensitivity (with mutations Q111R and N122D) (27) for the selective inhibition of the endogenous Na$^+$/K$^+$-ATPase as well as the sheep β_1-subunit were subcloned into vector pTLN as described (22, 23).

Oocytes were obtained by collagenase treatment after partial ovarectomy from *Xenopus laevis* females and were injected with 25 ng of α-subunit and 1 ng of β-subunit cRNA, which was prepared using the SP6 mMessage mMachine kit (Ambion, Austin, TX). After injection, oocytes were kept in oocyte Ringer's buffer (90 mM NaCl, 2 mM KCl, 2 mM $CaCl_2$, and 5 mM MOPS, pH 7.4) containing 1 mg/ml gentamycin at 18 °C for 4–6 days before measurements.

Oocyte Pretreatment and Fluorescence Labeling—Immediately before measurements, oocytes were incubated for 45 min in loading buffer (110 mM NaCl, 2.5 mM sodium citrate, and 10 mM MOPS/Tris, pH 7.4) and 15 min in post-loading buffer (100 mM NaCl, 1 mM $CaCl_2$, 5 mM $BaCl_2$, 5 mM $NiCl_2$, and 10 mM MOPS/Tris, pH 7.4) to elevate the intracellular Na$^+$ concentration (28). Cysteine-specific fluorescence labeling was achieved by incubating Na$^+$-loaded oocytes in post-loading buffer containing fluorescein-5-maleimide (FM), and/or TMRM (Invitrogen) for 30 min on ice in the dark followed by washes in dye-free buffer. For single-fluorophore labeling experiments, the oocytes were incubated in 5 μM the appropriate fluorophore. For double-fluorophore labeling experiments, the oocytes were incubated with 1 μM FM and 4 μM TMRM. At this fluorophore ratio and assuming that each fluorophore reacts with cysteine at the same rate, it is predicted that an ion pump with two cysteine residues will be labeled pairwise at the following proportion: 4% FM:FM (D:D), 32% FM:TMRM (D:A), and 64% TMRM:TMRM (A:A). For the

subsequent donor photobleaching experiments, the predominant measured species will be the FM:TMRM pair as the TMRM:TMRM pair will be excluded through the usage of the correct filters (described below). However, there will be a small population of ion pumps that are labeled with two donor fluorophores. This population will induce a faster observed decay rate, and therefore, the distance measurements could be slightly under-calculated.

Measurements for TMRM under Na^+/Na^+ exchange conditions were performed in Na^+ test solution (100 mM NaCl, 5 mM $BaCl_2$, 5 mM $NiCl_2$, 10 μM ouabain, and 10 mM MOPS/Tris, pH 7.4) with continuous solution flow. FM measurements, under Na^+/Na^+ exchange conditions, were performed in Na^+ test solution without $NiCl_2$. For stationary pump current recordings, 10 mM NaCl was replaced with an equimolar amount of KCl.

Two-electrode Voltage Clamp Epifluorescence Measurements—An oocyte perfusion chamber was mounted on the stage of a fluorescence microscope (Axioskop 2FS, Carl Zeiss, Jena, Germany) equipped with a ×40 water immersion objective (numerical aperture: 0.8). Currents were measured using a two-electrode voltage clamp amplifier CA-1B (Dagan Instruments, Minneapolis, MN). Fluorescence was excited by a 100-watt tungsten lamp. Solution flow was constant to eliminate artifacts arising from a light-induced temperature change. The following optical filter components were used: TMRM (525AF45 excitation filter, 565ALP emission filter, and 560DRLP dichroic mirror), FM (475DF40 excitation filter, 530DF30 emission filter, and 505DRLP dichroic mirror), and FRET (475AF40 excitation filter, 595AF60 emission filter, and 505DRLP dichroic mirror) (all filters were obtained from Omega Optical, Brattleboro, VT). Fluorescence was measured with a PIN-022A photodiode (United Detector Technologies, Baltimore, MD) mounted to the microscope camera port. Photodiode signals were amplified by a patch clamp amplifier EPC-5 (HEKA Electronics, Lambrecht Germany). Fluorescence and current signals were simultaneously recorded and subsequently analyzed with Clampex 8.0 (Molecular Devices, Sunnyvale, CA) and Origin 7.5 (OriginLab Corp., Northampton, MA), respectively.

FRET and Anisotropy Measurements—For FRET distance measurements, oocytes expressing the Na^+/K^+-ATPase with two cysteine residues (one on both the α- and the β-subunits) were labeled with FM and/or TMRM as described previously in this report. Expression of the construct was verified with stationary pump current recordings, and the rate of donor photobleaching was monitored following illumination. The results of 4–6 oocytes were averaged, and the traces were usually fit to a monoexponential function. In some cases, traces were best fit by a biexponential function where the time constant corresponding to the fast component was used and the slow time constant was only a small fraction of the total decay (20). The origin of the smaller slow component is unknown. However, it could be due to a diffusion process on the plasma membrane of the oocyte. To determine the efficiency of energy transfer (E), the following equation was used: $E = 1 - \tau_{DA}/\tau_D$ (where τ_{DA} and τ_D are the time constants of donor photobleaching in the presence and the absence of acceptor, respectively) (29). FRET efficiency was converted to distance using the Förster equation: $E = 1/(1+ R^6/R_o^6)$, where R is the distance between the donor and acceptor and R_o is the distance corresponding to 50% efficiency for a specific donor-acceptor pair (29). R_o is defined by the equation: $R_o = (9.7 \times 10^3 \, J \, \Phi_D \, n^{-4} \, \kappa^2)^{1/6}$ (in Å), where J is the normalized spectral overlap of the donor emission and acceptor absorption, Φ_D is the donor emission quantum yield in absence of the acceptor, n is the index of refraction, and κ^2 is the orientation factor for a dipole-dipole interaction (30).

The anisotropy (r, Fig. 1*C*) of the donor and acceptor fluorophores was measured on the oocytes, which represent a quasi-planar system, and evaluated through the use of the following equation: $r = (I_{\parallel} - I_{\perp})/(I_{\parallel} + 2I_{\perp})$, where $I_{\parallel}$ is the parallel and $I_{\perp}$ is the perpendicular-emitted light with respect to the polarized excitation light at each amino acid (31, 32). The two components were measured sequentially with polarized filters (Linos Photonics, Inc., Göttingen, Germany) placed adjacent to the emission and excitation filters. To calculate the error in the distance measurements due to anisotropy, the following equations were used: $\kappa^2_{max} = 2/3(1 + F_{rd} + F_{ra} + 3\, F_{rd} \times F_{ra})$ and $\kappa^2_{min} = 2/3(1 - (F_{rd} + F_{ra})/2)$ where $F_{rd} = (r_d/r_o)^{0.5}$ and $F_{ra} = (r_a/r_o)^{0.5}$; r_d is the anisotropy of FM, r_a is the anisotropy of TMRM, and r_o is the fundamental anisotropy of each fluorophore (FM: 0.4 and TMRM: 0.38) (18, 33).

RESULTS

Expression and Labeling Experiments—Our group has shown that following single-cysteine mutagenesis on the M5-M6 loop of the α-subunit and on the transmembrane-cytosolic interface of the β-subunit, the ion pump is active, and that the stationary currents can be directly attributed to the ouabain-insensitive form of the Na^+/K^+-ATPase (22, 23, 27). Additional single- and double-cysteine constructs of the Na^+/K^+-ATPase that contained a cysteine mutation on the M3-M4 loop or double-cysteine mutants (one cysteine mutation on both the α- and the β-subunits) were examined for activity. Functional expression was demonstrated by measuring stationary pump currents upon the addition of 10 mM K^+ in two-electrode voltage clamp experiments in the presence of 10 μM ouabain to inhibit the endogenous Na^+/K^+-ATPase of the oocytes. All constructs were functional and produced currents similar to the cysteine-less construct, which gave the same results as the ouabain-insensitive wild-type construct (Fig. 1*D*). Each construct could also be largely inhibited upon the application of 10 mM ouabain (not shown). Complete inhibition cannot be achieved by 10 mM ouabain because of the half-maximal inhibition value (~2 mM) for the ouabain-resistant Na^+/K^+-ATPase used in these studies (34). However, the transport activity could be directly attributed to the ouabain-resistant Na^+/K^+-ATPase constructs (27).

Intermolecular FRET Analysis—Fluorescence labeling of specific residues of the Na^+/K^+-ATPase has previously provided insight into the conformational dynamics of the ion pump during the transport cycle where the fluorescence intensity can be correlated to the conformational state of the ion pump and the kinetics of fluorescence change can be compared with ion transport across the plasma membrane (22, 23). Our current aim, however, is to investigate the relative conformational dynamics between the α- and β-subunits of the ion pump

by labeling both subunits with fluorophores and monitoring changes in FRET.

Our first objective, therefore, was to determine whether there was significant FRET between two α-subunits or two β-subunits of the ion pump in the *Xenopus* oocyte plasma membrane. The results from this experiment would answer two questions. First, it would provide insight into the α/β-stoichiometry of the Na^+/K^+-ATPase in the plasma membrane, and second, it would determine whether the measurement of distance constraints between the α- and β-subunits would be feasible as a large intermolecular FRET component, between two α-subunits or two β-subunits, would complicate data analysis. Therefore, three single-cysteine constructs, αT309C (located on the extracellular loop between M3 and M4 on the α-subunit), αN790C (located on the extracellular loop between M5 and M6 on the α-subunit), and βS62C (located adjacent to the transmembrane domain on the β-subunit) were selected for labeling. It has previously been shown that the conformational state of the ion pump can be monitored following labeling with TMRM at each of these sites during solution exchange (with Na^+ or K^+) and/or voltage-pulses (22, 23, 35). These constructs were concurrently labeled with the donor fluorophore (FM) and the acceptor fluorophore (TMRM). Energy transfer was analyzed by measuring the change in intensity of the acceptor fluorophore following excitation of the donor fluorophore under Na^+/Na^+ exchange conditions. These conditions enable precise regulation of the two main conformational states of the ion pump by controlling the membrane potential of the cell (36). In these experiments, we are not directly investigating the conformational state of the protein; instead, the change in fluorescence intensity is identifying whether the donor fluorophore is close to the acceptor fluorophore. Preliminary experiments have established that following FM labeling of αT309C, αN790C, and βS62C, changes in fluorescence were observed during shifts in membrane potential (not shown). Therefore, when two cysteine residues are labeled with FM and TMRM and they are within the Förster radius, a change in FRET intensity would be observed during voltage pulses. These results from the single-cysteine constructs were compared with the emission of the acceptor fluorophore when the double-cysteine constructs αT309C/βS62C and αN790C/βS62C were labeled with both donor and acceptor fluorophores.

The single-cysteine constructs, with a stationary current of greater than 100 nA, demonstrated low levels of FRET, where the total change of fluorescence for these constructs was equal to or less than 0.5% of the total fluorescence (Fig. 2, *A*–*C*). In contrast, the double-cysteine (one cysteine mutation on both the α- and the β-subunits) constructs, with a stationary current of greater than 100 nA, exhibited fluorescence changes that were greater than 3% (Fig. 2, *D* and *E*). Thus, there is only a low amount of energy transfer between α-α- or β-β-subunits in the oocyte expression system. The observed residual FRET response for the single-cysteine mutant constructs is most likely due to the high density of ion pumps on the cell surface, which causes a small population of ion pumps to be within the Förster radius in the plasma membrane. In contrast, the double-cysteine constructs display a significant α-β energy transfer component, and therefore, the results from this experiment do not support the presence of a dimeric or higher order structure of the Na^+/K^+-ATPase in the plasma membrane of the *Xenopus* oocyte. Therefore, it is possible to measure distances between the α- and β-subunits.

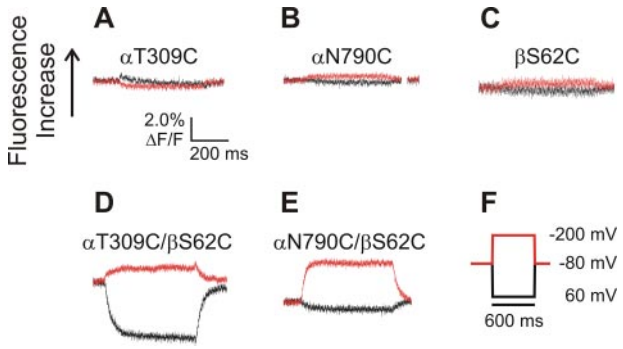

FIGURE 2. Voltage pulse-induced fluorescence responses from oocytes expressing αT309C (*A*), αN790C (*B*), βS62C (*C*), αT309C/βS62C (*D*), and αN790C/βS62C (*E*). All oocytes demonstrated a robust stationary pump current (>100 nA) and were concurrently labeled with FM and TMRM (1:4 ratio). FRET responses were measured following selective excitation of FM and selective measurement of TMRM emission. *F* shows the applied voltage protocol. The observed change in TMRM fluorescence as a function of membrane potential is the cumulative result of the change in fluorescence of the donor (FM) and acceptor (TMRM) fluorophores.

Anisotropy Measurements—Uncertainties in anisotropy and subsequent κ^2 calculations can lead to errors in the estimation of R_o for a donor/acceptor pair since residues that exhibit significant polarized emission can affect the amount of energy transfer between the donor and acceptor fluorophores, and therefore, influence the distance measurements, which are derived from irreversible fluorophore bleaching measurements (32). Therefore, the relative mobility of FM and TMRM was determined using polarized filters under Na^+/Na^+ exchange conditions (Fig. 1*C*). At each of the residues examined, both fluorophores were highly mobile. Following the subsequent calculation of κ^2, the range of κ^2 for the αT309C/βS62C double mutant was 0.4–1.5, whereas the range for the αN790C/βS62C double mutant was determined to be 0.4–1.6. As the anisotropy measurements indicated that all of the residues had a reasonable mobility, κ^2 was assumed to be 2/3 (18–20). Therefore, R_o was estimated for the FM/TMRM pair to be 55 Å (20).

Our group has demonstrated that specific residues labeled with TMRM undergo fluorescence changes as a function of solution exchange, but it has remained unknown whether the fluorescence changes are the result of a change of the environment surrounding the fluorophore or are the result of a reorientation of the fluorophore (22, 23, 35). To examine the relative orientation of the fluorophores, polarized light was used to excite TMRM in the E_1 (K^+ external solution) and E_2 (Na^+ external solution) conformation. The amount of parallel and perpendicular emitted light was measured with polarized filters (Fig. 1*C*). No significant change in polarized emission was observed at any of three residues labeled with FM or TMRM in the E_1 or E_2 conformation. Therefore, the difference in the intensity of fluorescence following solution change is not the result of a change in anisotropy. The change in fluorescence is the result of a change in environment of the fluorophore.

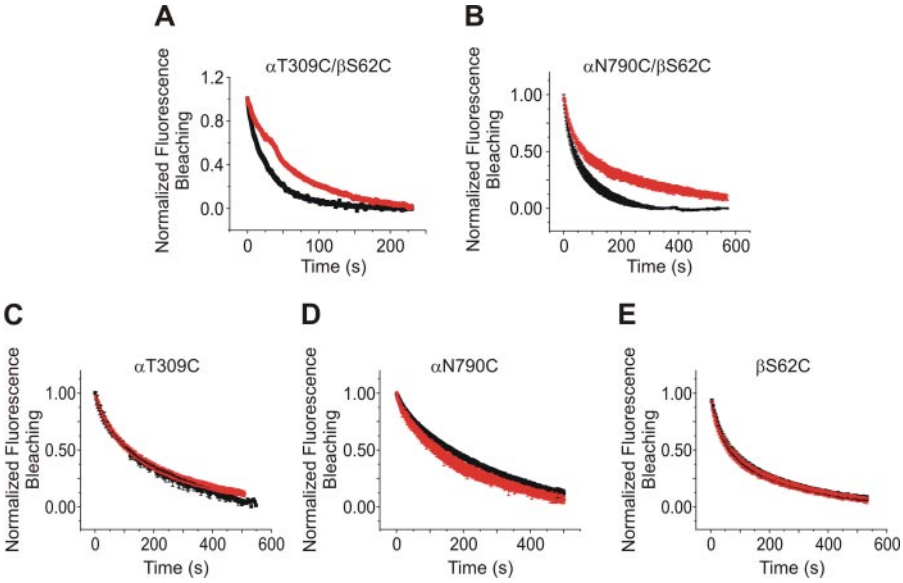

FIGURE 3. **Distance measurement of FRET efficiency by irreversible fluorophore bleaching.** *A–E*, photobleaching of the normalized ΔF_{donor} for the Na^+/K^+-ATPase with cysteine mutants: αT309C/βS62C (*A*), αN790C/βS62C (*B*), αT309C (*C*), αN790C (*D*), and βS62C (*E*) labeled with donor fluorophore alone (*black line*) or donor plus acceptor fluorophore in a 1:4 ratio (*red line*). For *A* and *B*, if both the donor and the acceptor fluorophores bind at the same rate at each residue (the chemistry is identical), the fluorophore ratio of double-cysteine constructs, DD:DA:AA, would be: 0.04:0.32:0.64 (see "Experimental Procedures" for details). The main component (A:A) is not observed due to the filters used during donor fluorophore photodestruction. The majority of fluorophores measured during donor fluorophore photodestruction would be the D:A pair. If the acceptor fluorophore binds at a faster rate, the total population of A:A will increase, whereas D:A and A:A will decrease proportionally, having a negligible effect on the distance measurements. If the donor fluorophore binds at a faster rate, increasing the relative proportion of D:D when compared with D:A, the measured distances could be affected and would result in a faster decay rate and a calculated distance that is smaller than the actual distance. As it turns out, if the relative proportion of D:D when compared with D:A increases, what will be observed is a faster decay rate, which translates into an observed distance that is smaller than the actual distance (for further details, see "Experimental Procedures"). The results are the mean of 4–6 oocytes ± standard error. The photodestruction rates for αT309C/βS62C are 52.1 ± 0.1 s^{-1} for the donor only and 43.0 ± 0.2 s^{-1} for the donor in the presence of the acceptor. The photodestruction rates for αN790C/βS62C are 74.7 ± 0.2 s^{-1} for the donor only and 34.9 ± 0.2 s^{-1} for donor in the presence of the acceptor.

Intersubunit FRET Analysis—To determine distance constraints between the α- and β-subunits, ion pumps that contained two cysteine mutations, one on both the α- and the β-subunits, were concurrently labeled with the donor (FM) and acceptor (TMRM) fluorophores (αT309C/βS62C or αN790C/βS62C). To determine distances between two residues, the time dependence of donor bleaching was measured following labeling with the donor (FM) fluorophore in the presence or absence of the acceptor (TMRM) fluorophore. The observed photodestruction rate of the donor fluorophore depends on the donor cumulative excited lifetime. On a single-molecule level, the donor, when not paired to an acceptor fluorophore, has a long excited state lifetime, and therefore, on the macroscopic scale, photobleaches at a relatively fast rate (16). The excited state lifetime of the donor fluorophore is shortened in the presence of an acceptor fluorophore due to energy transfer, which allows the donor, on a single-molecule level, to undergo more excitation cycles before photodestruction and which subsequently yields a slower macroscopic photobleaching. Furthermore, donor-acceptor pairs that are close together demonstrate a slower photodestruction rate of the donor fluorophore in the presence of the acceptor fluorophore when compared with a set of fluorophore-labeled residues that are farther apart (20, 21, 32). The difference between the rate of the irreversible photodestruction of the donor fluorophore in the presence and absence of the acceptor fluorophore can be used to calculate the distance between the two fluorophores using the Förster equation (29).

The rate of decay of the donor fluorophore, in the presence or absence of an acceptor fluorophore, was therefore measured at a controlled membrane potential (−20 mV) to maintain a constant distance between subunits (Fig. 3). Each oocyte was tested for K^+-induced stationary currents, and only oocytes with a stationary current of greater than 100 nA were used for analysis. Each data set was normalized, averaged, and fit to a mono- or biexponential function. Distance measurements were calculated, through the Förster equation, by determining the rate of donor photodestruction. No significant difference in the decay time of donor photodestruction was observed for single-cysteine mutant constructs (αT309C, αN790C, or βS62C) that were labeled with and without the acceptor fluorophore (Fig. 3, *C–E*). According to Förster's equation, the decay time of the donor photodestruction in the presence or absence of the acceptor fluorophore can be used to calculate the distance constraints between the α- and β-subunits. For the two sets of residues examined in this study, the distances were calculated to be 65 ± 8 Å for αT309C/βS62C and 53 ± 3 Å for αN790C/βS62C (Fig. 3, *A* and *B*) (see "Experimental Procedures").

Relative Movement of the α- and β-Subunits during Ion Transport—Following the measurement of distance constraints, we were interested in resolving the relative movement of the α- and β-subunits during the E_2 to E_1 transition evoked by Na^+ and K^+ concentration changes. However, due to the relatively large error bars on the donor photodestruction measurements, only gross structural changes could be observed using this technique. Therefore, an alternative strategy was pursued.

Previously, single-cysteine constructs that are labeled with a fluorophore have been identified because the fluorescence intensity changes during the E_1 to E_2 transition, and the fluorescence change is inhibited by high concentrations of ouabain (22, 23). In addition, it has been determined that the fluorescence changes observed on the β-subunit are kinetically linked to the conformational changes of the holoenzyme, although it has not been possible to directly determine the relative movement of both subunits. However, in previous experiments, the majority (~80%) of single-

cysteine constructs investigated demonstrate no fluorescence changes during the E_1 to E_2 transition of the ion pump, and these constructs have not been further studied (22, 23). The absence of fluorescence change for these constructs has two possible explanations; either the residue is not accessible to the extracellular solution and cannot be labeled, or the residue is labeled with a fluorophore and there is no environmental change during the E_1 to E_2 transition. Thus, our strategy was to identify residues that were labeled with a fluorophore but were insensitive to the E_1 to E_2 transition and to follow changes in FRET intensity following fluorophore labeling of two of these residues.

To identify residues that are labeled but insensitive to the E_1 to E_2 transition on both subunits, double-cysteine mutant constructs were expressed where one residue is known to bind a fluorophore (*i.e.* demonstrates fluorescence changes during solution exchange that induce the E_2 to E_1 transition) and where it is unknown whether the second residue binds a fluorophore (*i.e.* no fluorescence changes during solution exchange). To investigate FRET between these residues, the constructs were subsequently labeled with donor (FM) and acceptor (TMRM) fluorophores. In these experiments, we are not measuring the relative movement of the two cysteine residues. Instead, one cysteine is used as a relay to transfer energy to the second residue. Only when both sites have a bound fluorophore will one be able to observe a fluorescence change that is the product of the environmental change of TMRM at one residue (Fig. 4*A*). It is irrelevant which of the two residues has a donor or acceptor fluorophore as each pairing will exhibit the same result. If, on the other hand, only one of the two residues is labeled, no change in fluorescence will be observed (Fig. 4*B*).

Following this strategy, the double-cysteine constructs of αL306C/βS62C, αT309C/βP66C, αI788C/βS62C, and αN790C/βP66C were expressed (Fig. 4, *C–F*). In previous reports, our group has determined that the αL306C, αI788C, and βP66C constructs are functional (Fig. 1*D*) and do not demonstrate a change in fluorescence intensity during the E_1 to E_2 transition following labeling with TMRM (22, 23, 35). In contrast, our laboratory has shown that αT309C, αN790C, and βS62C demonstrate fluorescence changes during the E_1 to E_2 transition (22, 23, 35). Each of these double-cysteine constructs were labeled with both the donor and the acceptor fluorophores and exhibited a significant change in acceptor intensity following donor excitation upon the addition of 10 mM KCl, and the change in fluorescence intensity disappeared upon the addition of 10 mM ouabain, indicating that the fluorescence intensity change is directly attributed to the Na^+/K^+-ATPase (Fig. 4, *C–F*). Thus, it is clear that αL306C, αI788C, and βP66C are accessible to fluorophore labeling but that the fluorophores at these residues are insensitive to the E_1 to E_2 transition.

Therefore, the relative movement of the α- and β-subunits could be analyzed using these residues where the fluorescence intensity is insensitive to the E_1 to E_2 transition. As the distances between the sets of residues, previously determined by irreversible donor photobleaching, are close to R_o, this method will be highly sensitive to changes in distances between the two residues. Following labeling with both the

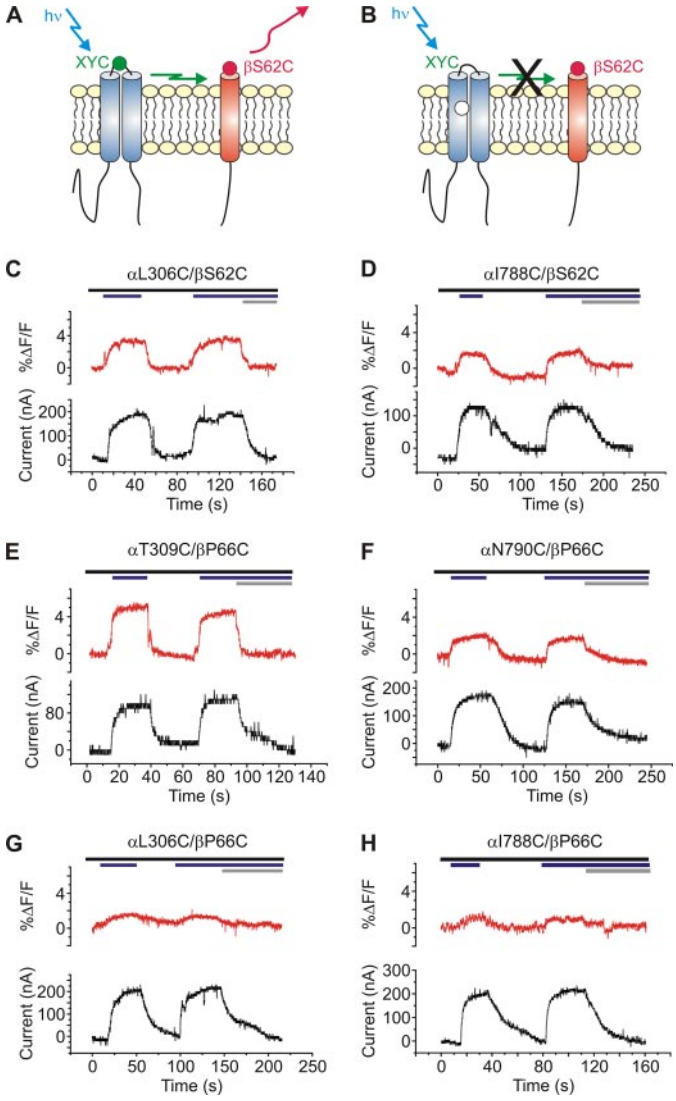

FIGURE 4. **Relative movement of the α- and β-subunits during ion transport.** Shown is a diagram of the method to identify fluorophore-labeled residues for double-cysteine constructs with two (*A*) and one (*B*) accessible cysteine residues. *A* and *B*, stationary pump currents of Na^+/K^+-ATPase double-cysteine mutants at −40 mV under Na^+/Na^+ exchange conditions (*black bars*) in response to 10 mM K^+ (*blue bars*) and 10 mM ouabain (*gray bars*). *C–H*, parallel recording of pump current (*lower*, *black*) and fluorescence resonance energy transfer change (*upper*, *red*) from oocytes expressing αL306C/βS62C (*C*), αT309C/βP66C (*D*), αL306C/βP66C (*E*), αI788C/βS62C (*F*), αN790C/βP66C (*G*), and αI788C/βP66C (*H*). Results are from a single oocyte, but the experiments were repeated, with essentially identical results, on at least four occasions.

donor and the acceptor fluorophores for the double-cysteine conformationally insensitive constructs, an increase in acceptor intensity following solution exchange would indicate that the two residues are moving toward each other, whereas a decrease in acceptor intensity would indicate that the two residues are moving away from each other. No change in intensity would indicate that the relative distance of the two residues is constant.

Both double-cysteine conformational-insensitive constructs (αL306C/βP66C and αI788C/βP66C) were functional (Fig. 1*D*), and following the application of 10 mM K^+, a small increase in acceptor FRET intensity was observed (Fig. 4, *G* and *H*). This result is directly attributable to the Na^+/K^+-ATPase as

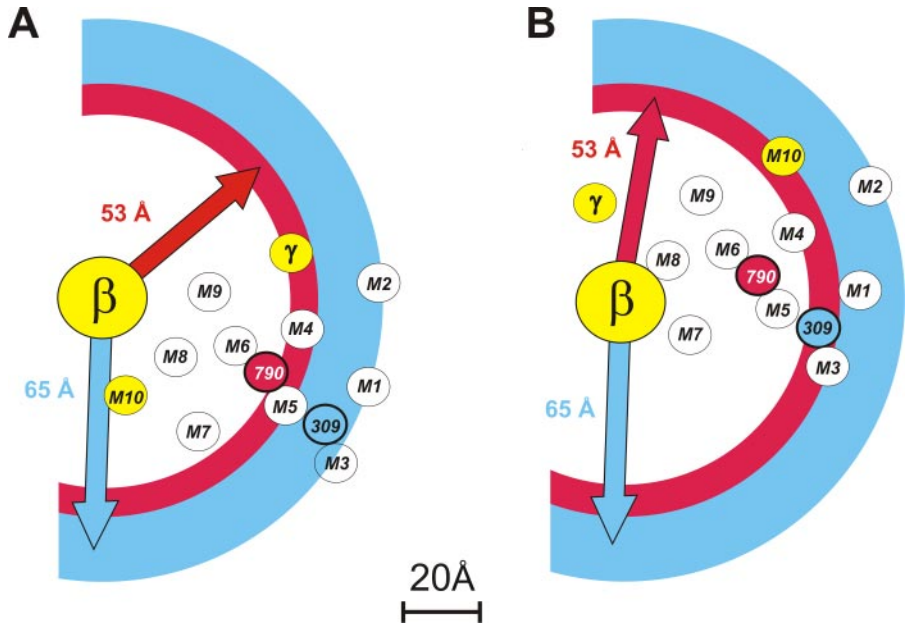

FIGURE 5. **Two-dimensional helix arrangement viewed from the surface of the cell as proposed by Hebert *et al.* (*A*) (13) and Jørgenesen *et al.* (*B*) (2).** The *scale bar* represents 20 Å. The orientation in *A* is based on electron microscopy studies of the Na^+/K^+-ATPase and assumes that the topology of the Na^+/K^+-ATPase is the same as the SERCA pump. The orientation in *B* is based on protein-protein interactions observed between the β-subunit and the M8 transmembrane domain of the α-subunit (15, 37) as well as chemical labeling of extracellular loops of the Na^+/K^+-ATPase (26). In both models, the relative distances between the transmembrane domains is derived from electron microscopy experiments (13). The distances in each part are derived from the donor photodestruction measurements. The width of the semicircles includes the error from these measurements.

the FRET intensity change is abolished following the addition of 10 mM ouabain. Thus, these data provide evidence that there is a conformational rearrangement between the α- and β-subunits during the E_2 to E_1 transition.

One concern regarding these experiments is that the change in fluorescence is the result of a small amount of FRET between two holoenzymes as opposed to between two subunits of one ion pump. However, it has been observed (Fig. 2, *A–C*) that the amount of FRET between two ion pumps is extremely small, and therefore, the change in fluorescence observed should be the result of the two subunits moving toward each other during the E_2 to E_1 transition.

Another possibility is that the change in FRET is due to a change in the orientation of the donor or acceptor fluorophore dipoles between the E_1 and E_2 conformations and not due to a change in the distance between the two fluorophores. However, as there is no significant change in anisotropy for either FM or TMRM at any of the residues tested in either external Na^+ or external K^+ solution, the change in FRET intensity is most likely due to a change in distance between the α- and β-subunits. (Fig. 1*D*).

DISCUSSION

The results from this study provide information on the relative orientation and movement of the α- and β-subunits of the Na^+/K^+-ATPase during ion transport. Previously, through the electron microscopy studies of Hebert *et al.* (13) and subsequent homology analysis with the SERCA pump, it was proposed that the β-subunit was located within the M9-M8-M10 pocket (Fig. 5*A*). More recently, it has been noted that this model does not explain additional data in the literature. A tryptophan scanning mutagenesis study of the β-subunit proposed that at least two faces of the β-subunit transmembrane helix affect the transport kinetics of the Na,K-ATPase (15). In addition, it has been observed that the β-subunit transmembrane helix and the M8 domain can be cross-linked (37). As the model proposed by Maunsbach and co-workers (13) only shows one face of the β-subunit adjacent to the α-subunit and a large distance between the M8 domain of the α-subunit and the β-subunit, an alternative structure was proposed where the β-subunit is located adjacent to M8 and close to M7 (2, 15, 37). In this model, the distances between the β-subunit and M3-M4 and M5-M6 loops are ~30 and 50 Å, respectively (Fig. 5*B*). In contrast, in the structure proposed by Hebert *et al.* (13), the approximate distances are 55 and 65 Å, respectively (Fig. 5*A*). Thus, the distances obtained from our analysis agree with the structure by Hebert *et al.* (13) where the β-subunit is adjacent to the M9-M8-M10 pocket (Fig. 5*A*).

It is important to note that all of the distance measurements have been interpreted in a two-dimensional model by assuming that the residues are located in the same plane parallel to the cell membrane. As both the M3-M4 and the M5-M6 loops are only six residues long and the residue from the β-subunit is proposed to be adjacent to the plasma membrane according to hydropathy analysis, it seems reasonable that the residues are on the same plane in relation to the plasma membrane. If, however, residues are located at different distances from the membrane surface, then the FRET measurements will overestimate the intersubunit distances, and the residues will seem farther apart in our model when compared with a true three-dimensional model. If this is to be the case, in order for the β-subunit to be adjacent to the M8 loop, large extracellular M3-M4 and M5-M6 loops would be required, which, as mentioned above, are not present.

One assumption during these experiments is that each fluorophore, which contains the same reactive group (maleimide), will react at each cysteine at an equivalent rate. However, it is possible that one fluorophore will react at a faster rate than the other. If the acceptor fluorophore reacts at a faster rate than the donor fluorophore at one or both cysteine residues, the total population of ion pumps that are labeled with two acceptor fluorophores (A:A) will increase, whereas the total population of ion pumps that are labeled with one donor and one acceptor (D:A) or with two donor

fluorophores (D:D) will decrease. As the A:A-labeled ion pumps do not influence donor photodestruction measurements, there will be no significant change in the measured distance. In contrast, if the donor fluorophore binds at a faster rate, the relative proportion of D:D when compared with D:A will increase, and a faster decay rate will be observed. This translates into a smaller calculated distance than the actual distance. Even if this is the case, the Jorgensen model would not be preferred over the Hebert model (Fig. 5) (2).

As a result of the electron microscopy studies, it has been proposed that the ion pump could form a multimeric complex as multiple contacts were observed in the electron microscopy studies between monomeric units. In these experiments, it was observed that the β-subunit of two monomeric units were in close proximity. However, our experiments do not support this interaction as no significant FRET is observed between multiple β-subunits (Figs. 2*C* and 3*C*).

A second contact between two monomeric units was also observed in the electron microscopy study (13). In this instance, the γ-subunit, which is located adjacent to the M2-M4-M9 pocket (Fig. 5*A*), is next to the M3-M5-M7 pocket of a neighboring ion pump. However, the results from our experiments are not able to confirm or reject this interaction.

In contrast to the static representations of the electron microscopy studies, our studies can be used to obtain insight into the relative movement of the α- and β-subunits during ion translocation. Previously, following trypsin digests of the ion pump, it was concluded that the extracellular domain of the β-subunit undergoes a conformational rearrangement during the E_2 to E_1 transition (38). However, the relative movement of the α- and β-subunit transmembrane domains during ion translocation remains unknown. By identifying residues proximal to the membrane interface of both subunits, where the fluorescence intensity is insensitive to the conformational dynamics of the holoenzyme, one can study the relative movement of specific residues on the transporter following labeling with donor and acceptor fluorophores. It was observed that a small increase in FRET efficiency between the α- and β-subunits is observed during the E_2 to E_1 transition. This small but significant increase in FRET efficiency indicates that the α- and β-subunits are moving toward each other during the E_2 to E_1 transition. Furthermore, the results from the anisotropy experiments indicate that the change in fluorescence during voltage pulses or solution exchange is not caused by changes in orientation of the fluorophore (22, 23, 35).

We have previously observed that the K65C mutation on the β-subunit results in an increase in apparent affinity for extracellular Na^+ (23). As lysine is conserved among β_1 species isoforms, in contrast to neutral (threonine) or polar (valine) residues on the human β_2 and β_3 isoforms, we proposed that sequence differences between isoforms could provide an additional tool for the modulation of ion affinity. The results from the current study demonstrate that there is a dynamic interaction between the α- and β-subunits. Therefore, it would be expected that the relative movement of the α- and β-subunits would be affected by charged, neutral, or polar residues on the β-subunit. This could be the mechanism by which different isoforms have different properties on ion affinity.

Thus, from our measurements of distance constraints, we have been able to differentiate between two orientations of the β-subunit in relation to the α-subunit and have accumulated evidence that there is a structural rearrangement between the extracellular transmembrane region of the β-subunit and both the M3-M4 and the M5-M6 regions of the α-subunit during ion translocation. This study provides a framework by which small distance changes of membrane proteins can be observed on single cells by solution exchange.

Acknowledgments—We thank F. Fendler for excellent discussions and G. Ziffarelli for preliminary experiments as well as E. Kaindl and V. Pintschovius for excellent technical assistance.

REFERENCES

1. Kaplan, J. H. (2002) *Annu. Rev. Biochem.* **71,** 511–535
2. Jørgensen, P. L., Hakansson, K. O., and Karlish, S. J. (2003) *Annu. Rev. Physiol.* **65,** 817–849
3. Jørgensen, P. L., and Pedersen, P. A. (2001) *Biochim. Biophys. Acta* **1505,** 57–74
4. Geering, K., Theulaz, I., Verrey, F., Hauptle, M. T., and Rossier, B. C. (1989) *Amer. J. Physiol.* **257,** C851–C858
5. Jassier, F., Jaunin, P., Geering, K., Rossier, B. C., and Horisberger, J. D. (1994) *J. Gen. Physiol.* **103,** 605–623
6. Therien, A. G., Pu, H. X., Karlish, S. J., and Blostein, R. (2001) *J. Bioenerg. Biomembr.* **33,** 407–414
7. Axelsen, K. B., and Palmgren, M. G. (1998) *J. Mol. Evol.* **46,** 84–101
8. Toyoshima, C., Nakasaki, M., Nomura, H., and Ogawa, H. (2000) *Nature* **405,** 647–655
9. Toyoshima, C., and Nomura, H. (2002) *Nature* **418,** 605–611
10. Toyoshima, C., and Mizutani, T. (2004) *Nature* **430,** 529–535
11. Toyoshima, C., Nomura, H., and Tsuda, T. (2004) *Nature* **432,** 361–368
12. Sorensen, T. L. M., Moller, J. V., and Nissen, P. (2004) *Science* **304,** 1672–1675
13. Hebert, H., Purhonen, P., Vorum, H., Thomsen, K., and Maunsbach, A. (2001) *J. Mol. Biol.* **314,** 479–494
14. Rice, W. J., Young, H. S., Martin, D. W., Sachs, J. R., and Stokes, D. L. (2001) *Biophys. J.* **80,** 2187–2197
15. Hasler, U., Crambert, G., Horisberger, J. D., and Geering, K. (2001) *J. Biol. Chem.* **276,** 16356–16364
16. Mannuzu, L. M., Moronne, M. M., and Isacoff, E. Y. (1996) *Science* **271,** 213–216
17. Cha, A., and Bezanilla, F. (1997) *Neuron* **19,** 1127–1140
18. Cha, A., and Bezanilla, F. (1998) *J. Gen. Physiol.* **112,** 391–408
19. Koch, H. P., and Larsson, H. P. (2005) *J. Neurosci.* **25,** 1730–1736
20. Glauner, K. S., Mannuzu, L. M., Gandhi, C. S., and Isacoff, E. Y. (1999) *Nature* **402,** 813–817
21. Cha, A., Snyder, G. E., Selvin, P. R., and Bezanilla, F. (1999) *Nature* **402,** 809–813
22. Geibel, S., Kaplan, J. H., Bamberg, E., and Friedrich, T. (2003) *Proc. Natl. Acad. Sci. U. S. A.* **100,** 964–969
23. Dempski, R. E., Friedrich, T., and Bamberg, E. (2005) *J. Gen. Physiol.* **125,** 505–520
24. Albers, R. W. (1967) *Annu. Rev. Biochem.* **36,** 727–756
25. Post, R. L., Kume, S., and Hegyvary, C. (1972) *J. Biol. Chem.* **247,** 6530–6540
26. Hu, Y. K., and Kaplan, J. H. (2000) *J. Biol. Chem.* **275,** 19185–19191
27. Price, E. M., and Lingrel, J. B. (1988) *Biochemistry* **27,** 8400–8408
28. Rakowski, R. F. (1993) *J. Gen. Physiol.* **101,** 117–144
29. Forster, T. (1948) *Ann. Physik* **2,** 55–75

30. Van Der Meer, B. W., Coker, G., and Chen, S. Y. D. (1994) *Resonance Energy Transfer: Theory and Data*, John Wiley & Sons, Inc., New York
31. Dale, R., Eisinger, J., and Blumberg, W. (1979) *Biophys. J.* **26,** 161–194
32. Lakowicz, J. (1999) *Principles of Fluorescence Spectroscopy*, 2nd Ed., pp. 395–424, Kluwer Academic/Plenum Publishers, New York
33. Chen, R. F., and Bowman, R. L. (1965) *Science* **147,** 729–732
34. Horisberger, J. D., and Kharoubi-Hess, S. (2002) *J. Physiol.* (*Lond.*) **539,** 669–680
35. Zifarelli, G., Geibel, S., Bamberg, E., and Friedrich, T. (2003) *Biophys. J.* **84,** 268A
36. Nakao, M., and Gadsby, D. C. (1986) *Nature* **323,** 628–630
37. Or, E., Goldshlegger, R., and Karlish, S. (1999) *J. Biol. Chem.* **274,** 2802–2809
38. Lutsenko, S., and Kaplan, J. H. (1993) *Biochemistry* **32,** 6737–6743
39. Guex, N., and Peitsch, M. C. (1997) *Electrophoresis* **18,** 2714–2723